

## CONTRAST OPTIMISATION FOR BACKSCATTERED ELECTRON IMAGING OF RESIN EMBEDDED CELLS

L.G. Harris<sup>1</sup>, I. ap Gwynn<sup>2</sup> and R.G. Richards<sup>1\*</sup>

<sup>1</sup>Interface Biology, AO Research Institute, Davos, Switzerland.

<sup>2</sup>Institute of Biological Sciences, The University of Wales, Aberystwyth, Wales

(Received for publication May 19, 1998, and in revised form August 20, 1998)

### Abstract

Adhesions between cells and substrates can be observed when the undersurfaces of resin-embedded cells are examined using high emission current backscattered electron (HCBSE) imaging with a Field Emission Scanning Electron Microscope (FESEM). The aim of this study was to find a fixation procedure that would optimise the contrast of cell adhesion areas when observed at low beam energies as well as the nucleus and stress fibres of the cell cytoskeleton viewed at medium beam energies.

Balb/c 3T3 and L929 fibroblast cells were cultured on plastic discs, fixed and stained with one of six variant protocols, comprising of a variety of chemical fixatives, mordants and stains. Following dehydration the cells were embedded in acrylic resin. After the plastic discs were removed, the specimens were coated with Au/Pd, and examined in a FESEM using the HCBSE technique, at accelerating voltages of 4, 8 and 15 kV.

The application of fixation protocol variants resulted in obtaining different contrast levels of the adhesion areas. The addition of 0.1% OsO<sub>4</sub> to the primary fixative was beneficial to the cells' contrast, but the best results were obtained from the additional binding of osmium in the OTO method. The different focal adhesion organisation observed in Balb/c 3T3 and L929 cells may have resulted from different effects of the fixatives on the different cell types.

**Key Words:** Backscattered electron imaging, scanning electron microscopy, atomic number contrast, fibroblast cells, adhesion, undersurface.

### Introduction

It is known that cells need to be attached to neighbouring cells or to an extracellular matrix (ECM) of macromolecules for growth and survival. Due to the increase in the use of metal implants in bone fracture fixation, the factors influencing the interaction and adhesion of both the soft and hard tissue cells to these biomaterials are of interest to the medical world. Understanding how the cells adhere to implants would be advantageous to improving the biocompatibility of surfaces' and decreasing the possibility of infection.

Richards *et al.* (1997) developed a method to study directly the adhesion of cells to metallic implants using high emission current backscattered electron (HCBSE) imaging with the Field Emission Scanning Electron Microscope (FESEM) followed by image analysis. Fibroblast cells were cultured on either metallic implant substrates or 'Thermanox' plastic discs, then chemically fixed, stained with heavy metals, dehydrated and embedded in LR White acrylic resin. After the removal of the metal implant substrate (Richards *et al.*, 1995) or a Thermanox disc, the underside of the embedded cells were examined directly using HCBSE imaging with an FESEM (Richards and ap Gwynn, 1995). At a high beam energy (15 kV) the beam penetrates deep into the cell, revealing the cell's cytoskeleton and its general shape, while at a low beam energy (4 kV), the areas of cell attachment were observed. However, during the study it was observed that the stained adhesion areas of L929 fibroblastic cells were diffuse in comparison to the distinct stained areas of the Balb/c 3T3 fibroblast cells.

Image contrast for electron microscopy (EM) is provided, in chemically fixed biological specimens, by the heavy metal fixatives and stains incorporated during fixation procedures. Chemical fixations stabilise the structural organisation of cells or tissues such that ultrastructural relationships are preserved in an acceptable condition, despite the ensuing treatments of dehydration, embedding and exposure to the electron beam. Chemical fixations can be applied to specimens for morphological studies, though they are less useful for physiological studies, where cryo-fixation would probably be required. Sabatini *et al.* (1963), observed that treating a tissue with an aldehyde, particu-

\*Address for correspondence:

R.G. Richards

AO ASIF Research Institute,

Clavadelstrasse, CH 7270, Davos, Switzerland

Telephone Number: 0041 81 414 23 97

FAX number: 0041 81 414 22 88

E-mail : geoff.richards@ao-asif.ch

larly glutaraldehyde, followed by a secondary fixation with osmium tetroxide ( $\text{OsO}_4$ ) gave good results. This type of protocol has become generally accepted as being the best approach for the chemical fixation of biological tissues, for electron microscopy. However, other solutions of heavy metals, stains and additives can be added to the fixation procedure in order to enhance the preservation and contrast of the specimen.

Ruthenium red (ammoniated ruthenium oxy-chloride) is an inorganic, intensely coloured, crystalline compound, which acts as an oxidant and is added to  $\text{OsO}_4$  to enhance the staining of tissues (Luft, 1971). It forms a moderately heavy (atomic number 44) hexavalent cation, and reacts with anions. Sobota (1997) showed that ruthenium red enters cells forming globular structures on the cytoplasmic surface of the plasma membrane. When ruthenium red is used in combination with  $\text{OsO}_4$  the two compounds react to form ruthenium tetroxide. Ruthenium tetroxide reacts with many cellular components to provide enhanced contrast staining.

$\text{OsO}_4$  in combination with potassium ferricyanide ( $\text{K}_3\text{Fe}(\text{CN})_6$ ) has been used for enhancing contrast, staining of a wide variety of cellular components and has been known for a long time to preserve glycogen (De Bruijn, 1968). The  $\text{OsFeCN}$  mixture enhances electron-scattering capacity of cellular components compared to the use of  $\text{OsO}_4$  alone (McDonald, 1984), and reduces the electron-scattering capacity of ribosomes and nuclear chromatin (De Bruijn, 1973).

Thiocarbohydrazide (TCH) is a bipolar sulphur-containing osmiophilic reagent, used as a ligand to bind additional osmium to a site, thereby enhancing the contrast (Seligman *et al.*, 1966; Aoki and Tavassoli, 1981). The tissue, or cultured cells are post-fixed with  $\text{OsO}_4$ , then treated with excess saturated TCH. This results in one end of the TCH molecule attaching to the osmium already in the cell or tissue. When this is followed by a second exposure to  $\text{OsO}_4$ , more osmium binds to the other end of the TCH molecule. The whole method results in an increase in the contrast of tissue osmiophilic components, e.g., lipids (Seligman *et al.*, 1966). The principle of the method is known as the OTO method (osmium-thiocarbohydrazide-osmium).

Many fixation methods for EM use uranyl acetate as a stain to improve the appearance of structures by increasing their contrast (Watson, 1958). Uranyl acetate is a good general stain and fixative, reacting with both negatively and positively charged side-chains on proteins, and retaining phospholipids in the cells, particularly in membranes, during dehydration. Additives are used in fixation procedures to enhance cell component preservation and contrast. Tannic acid ( $\text{C}_{70}\text{H}_{52}\text{O}_{46}$ ), was introduced as an additive fixative by Mizuhira and Futaesaku (1972). The mordanting effect

is believed to help reduce subsequent extraction of cell components during dehydration and embedding (Simionescu and Simionescu, 1976), and enhances uranyl acetate staining. LaFountain *et al.* (1977) found that after tannic acid staining, isolated actin filaments and microfilaments of c 3T3 fibroblasts could be seen.

In the 1970s it was established that heavy metal staining methods, adapted from light microscopy and transmission electron microscopy (TEM), used together with BSE imaging allowed visualisation of structures at or below the surface of material prepared for the scanning electron microscope (SEM) (Abraham and DeNee, 1973; Becker and Sogard, 1979). The production of BSE increases proportionally to the average atomic number of the specimen (Palluel, 1947), giving an image that shows atomic number contrast. Hence, the more stain on a biological structure, the stronger the signal that will be available for detection. The aim of this study was to find a fixation procedure to optimise for BSE imaging, the contrast, of both cellular adhesion areas and the cytoskeletal stress fibres.

## Material and Methods

### Cell culturing

L929 and Balb /c3T3 fibroblastic cells (European Collection of Cell Cultures, Salisbury, UK) were maintained according to the method of Elvin and Evans (1982). Stock cultures were recovered from a liquid nitrogen refrigerator and were plated at 300 000 cells per 25cm<sup>2</sup> plastic flask in DMEM (Dulbecco's Modified Eagle's Medium) with 10% foetal calf serum, without antibiotics. After 3 days cells were detached with 0.25% trypsin and 0.02% EDTA (ethylenediaminetetraacetic acid) in TBSS (tyrode buffered saline solution) - calcium and magnesium free. Detached cells were recovered, rinsed and cultured on pre-sterilised polyethylene terephthalate (Thermanox) 13mm discs (Life Technologies, Basel, Switzerland) at an inoculum of 30 000 cells per well for 24 hours, not to confluency.

### Preparation for electron microscopy

Fixation was carried out at 20°C. The cell culture medium was removed and the cells were rinsed for 2 minutes in 0.1 mol l<sup>-1</sup> PIPES (Piperazine-NN'-bis-2-ethane sulphonic acid) buffer pH 7.4. The cells were primarily fixed in 2.5% glutaraldehyde (GA) in 0.1 mol l<sup>-1</sup> PIPES pH 7.4 for 5 minutes. The cells were rinsed three times for 2 minutes each in 0.1 mol l<sup>-1</sup> PIPES pH 7.4 before postfixation in 0.5% osmium tetroxide with filtered ruthenium red (375 ppm / 0.0375%) in 0.1 mol l<sup>-1</sup> PIPES pH 6.8 for 60 minutes. The cells were rinsed 3 times for 2 minutes each in double distilled water and stained with 5% aqueous uranyl acetate for 60 minutes. The above method was the control protocol. Other Balb/c 3T3 and L929 cells were fixed using the variants shown in Table 1.

**Table 1.** Fixation variants from the control.

Variant	PRIMARY FIXATION	SECONDARY FIXATION
Control	2.5% GA + PIPES	0.5% OsO <sub>4</sub> + Ruthenium Red (375ppm) + PIPES
1	Control + 0.1% OsO <sub>4</sub>	1% OsO <sub>4</sub> + Potassium ferricyanide + PIPES
2	Control + 0.1% OsO <sub>4</sub>	1% OsO <sub>4</sub> + PIPES
3	Control + 0.1% OsO <sub>4</sub>	1% OsO <sub>4</sub> + Ruthenium Red (375ppm) + PIPES
4	Control	Tannic acid (30min) => 1% OsO <sub>4</sub> + PIPES (1hr)
5	Control + CaCl <sub>2</sub>	OTO method

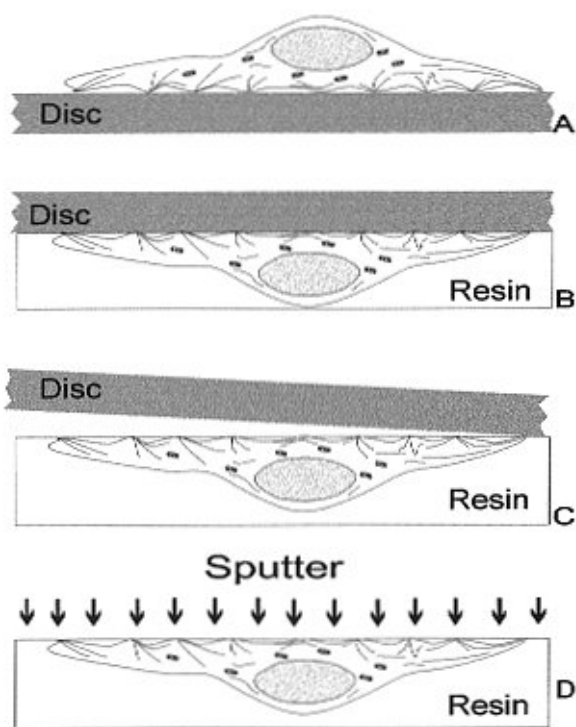


**Figure 1.** Cell preparation. (A) Culturing, fixation, staining and dehydration. (B) Resin impregnation, polymerisation and sample removal. (C) Removal of the Thermanox disc. (D) Sputter coating with 10nm Au/Pd.

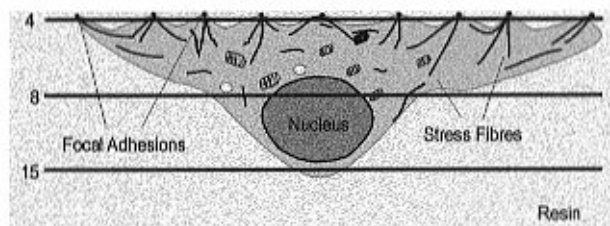


**Figure 2.** Cross-section of the cell-substrate interface, after the removal of the Thermanox disc. The three lines across the cell represent approximate depth from which BSE emerge at 4, 8 and 15 kV.

The OTO method (variant 5) entailed post-fixing cells, incubation in excess 1% thiocarbonylhydrazide (TCH) for 10 minutes, before fixing a second time with unbuffered OsO<sub>4</sub> for 30 minutes (Seligman *et al.*, 1966; Kelley *et al.*, 1973). The procedure used was otherwise the same as for the control protocol.

Each fixed cell culture was taken through an ethanol series of 50%, 70%, 96% and 100% for 5 minutes respectively, followed by LR White resin (London Resin Co., Basingstoke, UK) allowing 1 hour for infiltration into the cells. The discs were removed and placed, cell-side upwards, in 15 mm wells in a silicone rubber mould. Fresh resin was poured onto them and a drop of paraffin oil added on the surface, to exclude oxygen from the resin. The resin was cured thermally at 55°C for 16 hours. The polymerised resin blocks containing the cells were removed from the mould and excess resin was cleaned from the disc with abrasive paper, the discs being separated from the resin block with a sharp knife (Fig. 1). The embedded specimens were then mounted onto stubs and coated at a sputtering rate of 0.1 nm/s with 10nm of gold/palladium 80/20 (as measured with a quartz thin film monitor) in a Baltec MED020 unit (Balzers, Liechtenstein).

#### Microscope operating conditions

SEM examination of the specimens was performed with a Hitachi (Tokyo, Japan) S-4100 FESEM fitted with an Aurtara yttrium aluminium garnet (YAG) BSE detector (Prophysics, Uster, Switzerland) and a Quartz PCI image acquisition system (Quartz Imaging, Vancouver, Canada). The microscope was operated in HCBSE detection mode (Richards and ap Gwynn, 1995), to display the highly stained focal adhesion areas directly on the undersurface of the cells within the embedding resin. The microscope was operated at accelerating voltages of 15 kV, 8 kV and 4 kV respectively, all at 50µA emission current, which revealed information from different depths within the embedded cells (Fig. 2).

A working distance of 10mm was used to optimise both resolution and BSE collection. The condenser lens

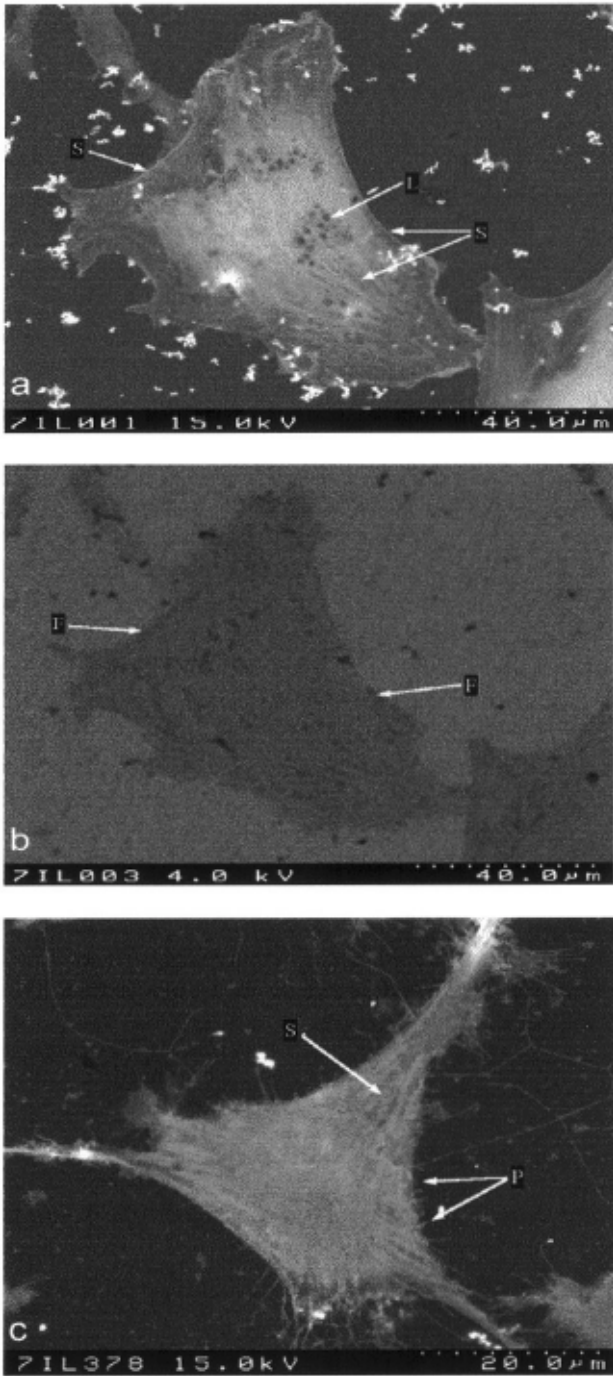


**Figure 3.** Image of a c-3T3 cell (control fixation). **(a)** At 15 kV (C18). Numerous stress fibres (S) are evident and non-stained saturated lipids (L). **(b)** At 4 kV (C12). In all cases observed at this accelerating voltage the images inverted. Faint traces of black focal adhesion areas (F) were observed, near the cell periphery. **(c)** 15 kV image of an L929 cell (control fixed) (C18). Many projecting filopodia (P) are present, in comparison to the c-3T3 cells. Some indistinct stress fibres (S) are observed.

current was maximised (setting C18), thus minimising the spot size. The widest objective aperture of 100 mm diameter (number 1) was used to allow more electrons to interact with the specimen. All images were stored in digital form.

## Results

The fixation variants used resulted in different contrast levels being obtained in images of the cells. At 15 kV, internal details of c-3T3 cells were clearly seen in most variants. However, the internal structures of L929 cells were not as well defined, and seemed to be obscured by the numerous filopodia on their surfaces. The stress fibres were evident in c-3T3 cells fixed by the control method, especially along the cell edges and traversing the cell (Fig. 3a). Structures that were probably saturated lipid droplets, which had not stained with the  $\text{OsO}_4$  were also observed between the stress fibres. The image inverted at 4 kV, but traces of focal adhesion areas were observed around the cell periphery (Fig. 3b). Many projecting filopodia were seen on the L929 cells, (fixed using the control method) when viewed at 15 kV, but few stress fibres were observed (Fig. 3c). No more cellular detail was seen when lower accelerating voltages were applied (not shown).

Variants 1, 2 and 3 had 0.1%  $\text{OsO}_4$  in the primary fixative, which resulted in the cells having more contrast than the control. The cells in variant 1 were post-fixed with solutions containing potassium-ferricyanide added to the  $\text{OsO}_4$ . This procedure produced poor contrast within the cells and there were signs of cellular components being extracted (not shown). Focal adhesion areas were not detected in either cell type when 4 kV was applied (not shown). Both cell types fixed with variant 2 were well contrasted, at all accelerating voltages. The nuclei of c-3T3 cells were stained to a greater extent than with any other treatment. Stress fibres, and other cytoskeletal components, were observed. What were probably accumulations of microtubules and intermediate filaments were also observed as a dense mass above and around the nucleus (Fig. 4a). At 4 kV the focal adhesion areas became detectable when the first condenser lens on the microscope was adjusted to give a very large spot size (Fig. 4b). Stress fibres and filopodia were observed in the L929 cells, when examined using 8 kV (Fig. 4c). Focal adhesion areas were detected around the peripheries of L929 cells, when observed at 4 kV (Fig. 4d). There was some damage to both the cells and the resin resulting from the preparation methods used.

After fixation with variant 3, both cell types exhibited good contrast. At an accelerating voltage of 15 kV, a dense network of stress fibres, which had taken up a considerable amount of stain, was clearly observed spanning the c-3T3 cell below the nucleus (Fig. 5a). The stress fibres travers-

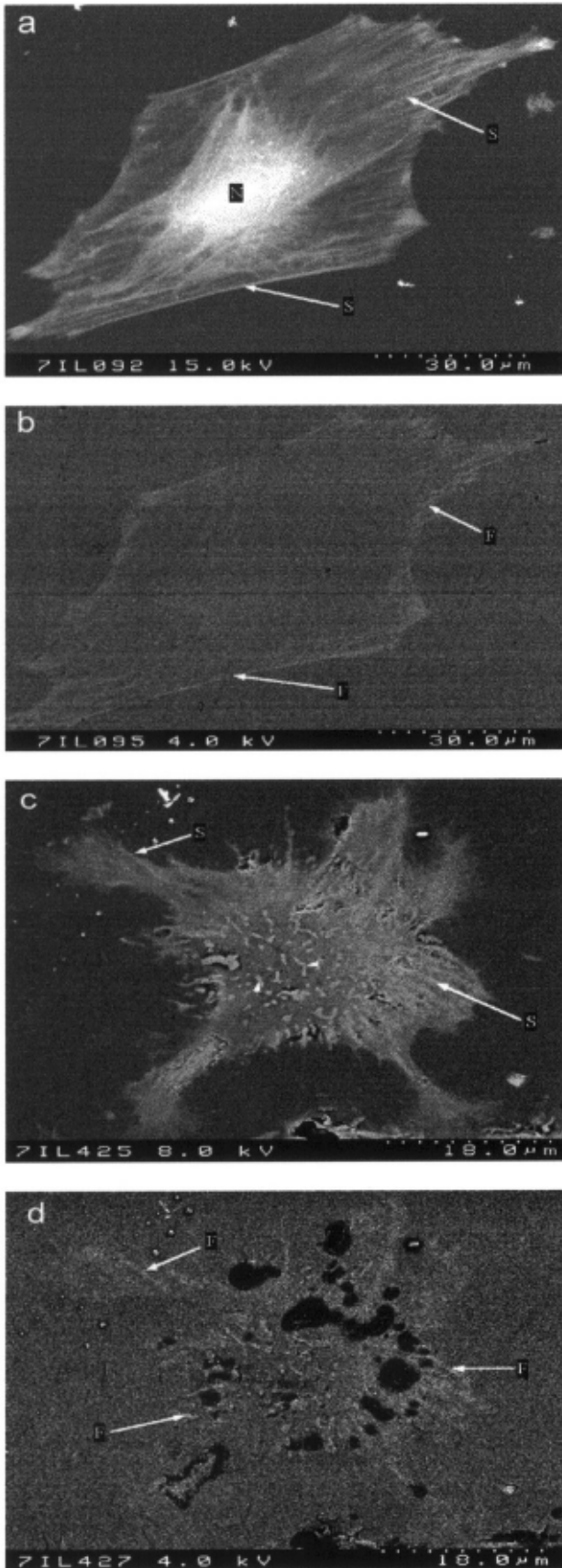


**Figure 4.** (a) 15 kV image (C18) of a c-3T3 cell (variant 2). The stress fibres (S) are stained well and a differentiation can be seen between the nucleus (N) and the rest of the cell. Around the nucleus are other cytoskeletal components, i.e., microtubules and intermediate filaments. (b) Image of the same cell at 4 kV (C8). Scattered focal adhesion areas (F) are visible, mainly at the end of the lamellipodia. (c) Image of an L929 cell (variant 2) at 8 kV (C18). Stress fibres (S) are seen bridging over the cell and along its edge. Filopodia like structures (arrows) are seen close to the surface, suggesting that they are attached to the disc. (d) Image of the same L929 cell at 4 kV (C13). Focal adhesion areas (F) are observed around the areas where lamellipodia and filopodia were seen at higher kV's.

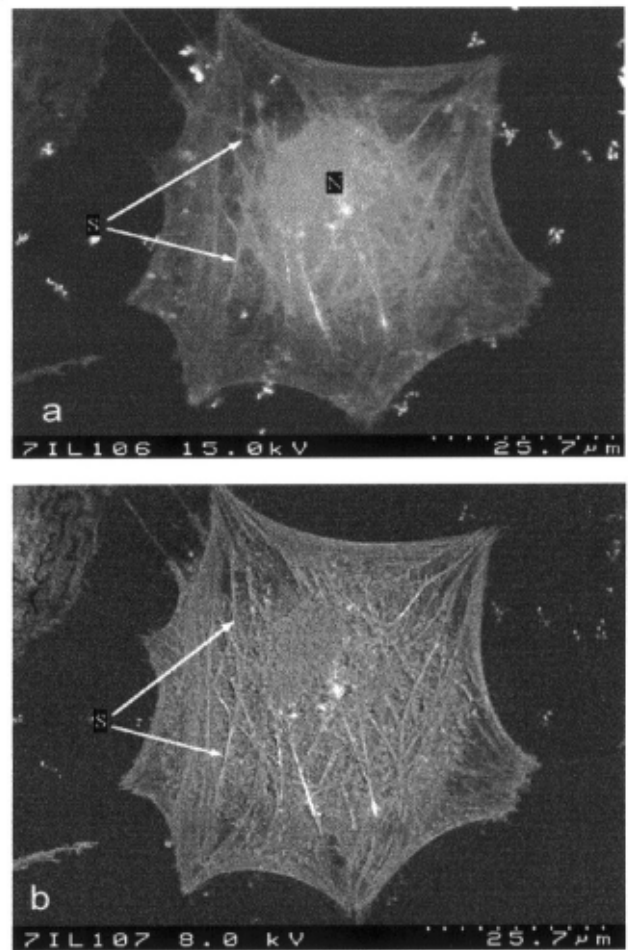


**Figure 5.** (a) 15 kV image of a c-3T3 cell (variant 3) (C18). The dense network of stress fibres (S) with good contrast, mainly cross below the nucleus (N). (b) The same cell imaged at 8 kV (C18). The stress fibres (S) are more apparent, traversing the cell and appear to converge at lamellipodia on the cell edge, where focal adhesion areas should be present.

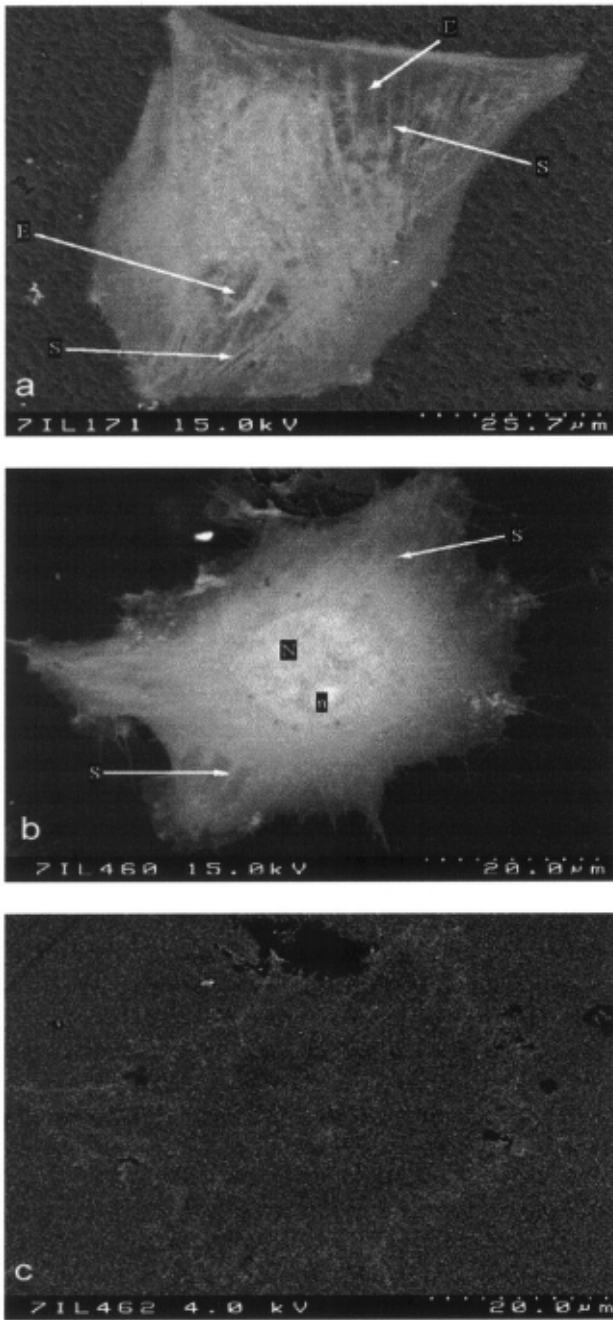


**Figure 6.** (a) 15 kV image (C18) of a well contrasted c-3T3 cell (variant 4). Stress fibres (S) are present and there is evidence of cytoplasmic extraction during the fixation (E). It may be, that the image is of one cell on top of another. (b) An L929 cell (variant 4) at 15 kV (C18). Diffuse appearing stress fibres (S) are observed towards the cell periphery. This is one of the few variants that show the nucleus (N), with a higher stained nucleolus (n). (c) The same L929 cell at 4 kV (C15). Faint focal adhesion areas are seen around the cell periphery.

ing the cell seemed to converge at different points along the cell edge at lamellipodia, indicating areas where focal adhesion areas should be found. At a lower accelerating voltage (8 kV), the stress fibres were more distinct (Fig. 5b). At 4 kV an inverted image of faint focal adhesion areas at the end of the lamellipodia were observed (not shown). At 8 kV stress fibres were observed in L929 cells, but were less distinct than within c-3T3 cells, and faintly stained adhesion areas were also just visible (not shown).

The addition of tannic acid to the fixation reagents (variant 4) resulted in well-contrasted c-3T3 and L929 cells, due to the high uptake of stain. Some diffuse stress fibres were observed crossing the c-3T3 cell in Figure 6a, but were not particularly clear at the cell edge. This may be due to them being hidden amongst a dense mixture of various cytoskeletal filaments and cytoplasmic structure. There was also some evidence near the edges that cytoplasm had been extracted during the fixation. In the L929 cell, observed at 15 kV, diffuse stress fibres, filopodia, a highly stained nucleus and what appeared to be unstained saturated lipids were seen (Fig. 6b). At 4 kV no adhesion areas were observed in c-3T3 cells (not shown), but some diffuse focal adhesion areas were visible in L929 cells (Fig. 6c).

Both cell types, when fixed with the OTO method (variant 5), exhibited good contrast (Figs. 7a-f). In the c-3T3 cell, the stress fibres were clearly seen towards the cell edge, and in particular traversing the cell along the lamellipodia (Fig. 7a). At 8 kV, the heavily stained stress fibres in the same cell as in Fig. 6a were well contrasted from the lesser-stained cytoplasm of the cell. The ends of the stress fibres were seen congregating at their lamellipodia ends while lower parts of the nucleus were also still detectable (Fig. 7b). This was the only variant that showed well-contrasted focal adhesion areas when examined at 4 kV (Fig. 7c). Stress fibres were also seen traversing the L929 cell, and unstained vesicles were observed in proximity to the nucleus, when examined using both 8 and 15 kV accelerating voltages (Fig. 7d and e). Focal adhesion areas were seen along the cell edge (Fig. 7f). Scattered in the area immediately surrounding the nucleus of both cell types a mass of white spots was observed. This indicated that some component of the cell (such as mitochondria) has taken up a considerable amount of heavy metal stain, or a compound had left a highly dense precipitate which had subsequently accumulated stain, for example,  $\text{CaCl}_2$  or TCH (Fig. 7a and d).

## Discussion

The amount of heavy metal stain introduced into the c-3T3 and L929 cells resulted in different levels of specimen contrast, which appeared to concentrate on the cells' internal structures, such as stress fibres and nuclei. By using different accelerating voltages, 'sections' of informa-

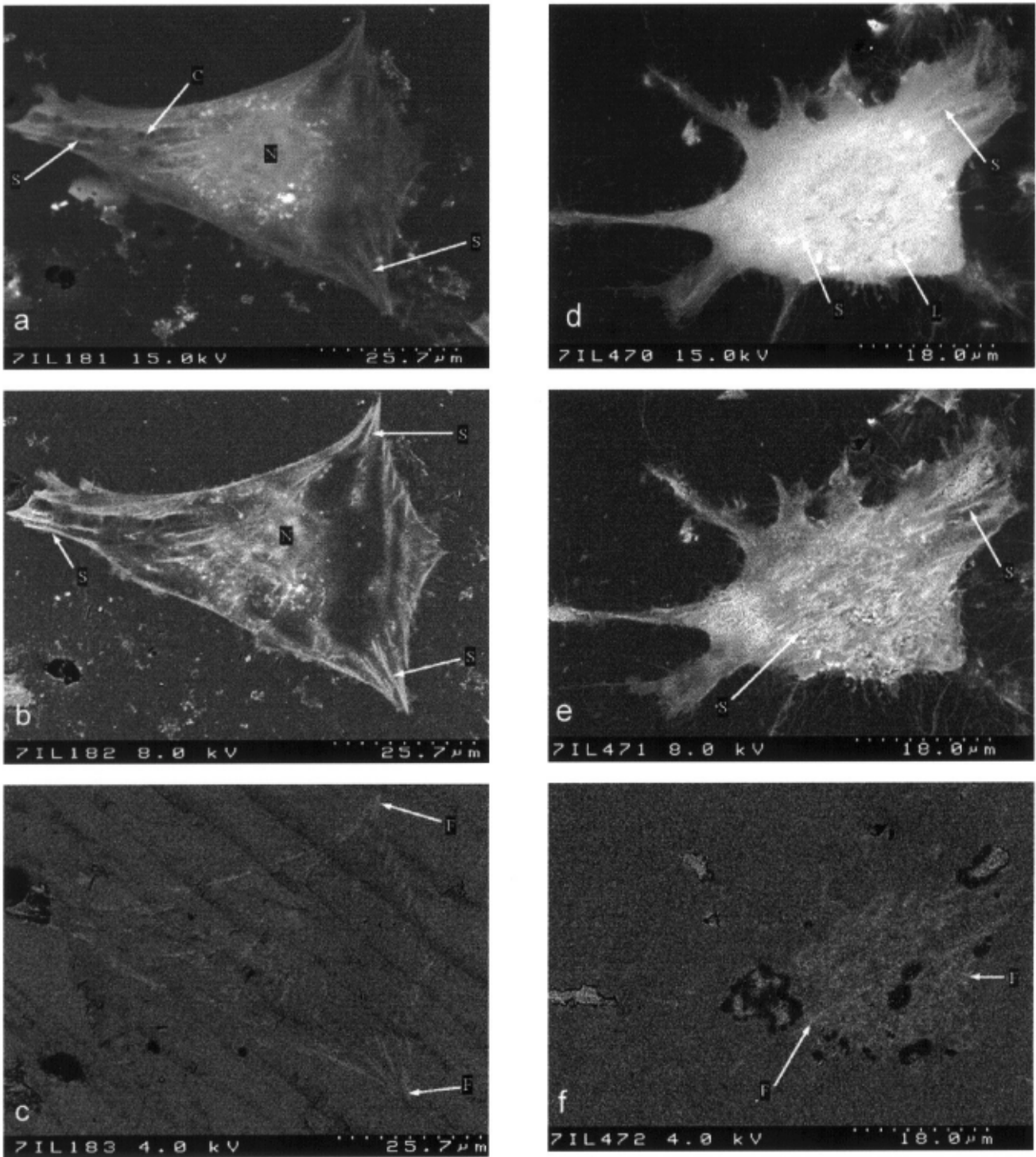


**Figure 7.** Images of a c-3T3 (a-c) and L929 (d-f) cell fixed with the OTO method. (a) At 15 kV (C18), the cell has good contrast. Stress fibres (S) are seen traversing along the lamellipodia with some cross-linking (C) between them. Around the nucleus (N) is a mass of unknown white stained spots. (b) At 8 kV (C18), ends of stress fibres (S) are seen at lamellipodia ends. Parts of the nucleus (N) are still visible. (c) At 4 kV (C15), stained focal adhesion areas (F) are seen around the cell edge where stress fibre termini had been seen at 8 kV. (d) At 15 kV (C18), stress fibres (S), nucleus (N) and unstained saturated lipids (L) are observed (e) At 8 kV (C18) stress fibres (S) are seen traversing the cell. Neither the nucleus nor saturated lipids are visible. (f) At 4 kV (C14), focal adhesion areas (F) are visible.

tion can be collected to give an overall insight into the three dimensional structure of the cell (Fig. 2). At 15 kV, the c-3T3 internal cellular details were clearly seen in most variants. However, the L929 internal cellular details were not as well defined, and seemed to be hidden behind the many filopodia on and around the cells. Within many of the cells (c-3T3 and L929), small spherical unstained bodies, probably saturated lipids, were observed. OsO<sub>4</sub> attaches to unsaturated lipids, but does not attach to saturated lipids (Glauert, 1975).

At high accelerating voltages (8 and 15 kV), most of the variants resulted in reasonably contrasted cells. Stress fibres, nuclei, and saturated lipids were normally observed. However at 4 kV, most of the cell images inverted, due to the limiting factors of the detecting system, the exception being those cells which had been fixed with the OTO method (variant 5). It is known that the production of BSE is strongly dependent on the atomic number differences within the specimen, and the variations in the number of BSE produced, results in an image. Hence, as the accelerating voltage decreases the backscatter coefficient (h) also decreases because fewer BSE emerge from the specimen, causing the image to invert (Goldstein *et al.*, 1992). Hence, the production of a BSE image is dependent on the use of heavy metals, particularly those with high atomic numbers, in the fixation procedure.

With the addition of ruthenium red to the secondary fixative (control) the contrast of c-3T3 cells was good, with many cellular structures seen at higher accelerating voltages (Fig. 3a). At 4 kV, the images inverted, but faint black areas of focal adhesion were observed around the cell periphery (Fig. 3b). The L929 cells exhibited less contrast, even when similar preparation procedures were applied, with few stress fibres observed at 15 kV (Fig. 3c). No cellular detail could be resolved at lower accelerating voltages.

Variant 1 had 0.1% OsO<sub>4</sub> in the primary fixative and potassium ferricyanide in the secondary fixative, a combination which is known to enhance the staining of microfilaments as well as the cell surface coat. However, both cell types showed poorly contrasted stress fibres. At 4 kV, the focal adhesion sites were seen as diffuse areas. A mixture of glutaraldehyde and OsO<sub>4</sub> in the primary fixation is believed to yield better preservation of cellular material (Trump and Bulger, 1966). Both cell types fixed with either variant 2 or 3, showed good contrast. A diffuse area of the cytoskeleton comprising of microtubules, intermediate filaments and microfilaments was seen in Figure 4a (variant 2). Such structures were not as clearly observed in other variants. In comparison to variant 1, well-defined stress fibres along the cell edges, and faint focal adhesion areas were seen at 4 kV. Hence the addition of OsO<sub>4</sub> to the primary fixative did result in improved contrast, as did adding ruthenium red to the secondary fixative (variant 3), because

of the extra heavy metal stain bound to the cellular structures.

Adding tannic acid to the fixatives resulted in both cell types showed good contrast (variant 4). However, stress fibres appeared diffuse, and no focal adhesion areas were seen in either cell type. It was possible that much of the contrast observed was due to the binding of uranyl acetate to the tannic acid (Hayat, 1989). The mordanting effect of tannic acid is believed to help reduce the extraction of cellular components during dehydration and embedding (Simionescu and Simionescu, 1976). However in the c-3T3s there appeared to be a large amount of cytoplasmic extraction present. This was probably due to over fixation (Figure 6a), or due to proteins conjugating during the fixation procedure. In general, the L929 cells appeared to be better preserved than the c-3T3 cells. The 'extraction' observed could also be the result of the electron beam penetrating through a thin area of the cell.

Variant 5 was based on the OTO method (Seligman *et al.*, 1966; Kelley *et al.*, 1973). The cell preservation obtained with this method was better in the c-3T3 cells than in L929 cells. The cells' contrast was probably good due to the additional OsO<sub>4</sub> binding to the TCH (Seligman *et al.*, 1966). The method also preserved other cell components well, particularly the stress fibres. A probable explanation for this was that the TCH's bridging activity between the two OsO<sub>4</sub> phases reduced the exposure of the cells to the OsO<sub>4</sub>, which can destroy the microfilaments (Aoki and Tavassoli, 1981). White precipitates or spots were observed around the nuclei of c-3T3 cells and some L929 cells, when observed at 15 kV. The identification of these structures is still unresolved, but they could be precipitates of calcium, OsO<sub>4</sub>, TCH, or any combination of these, since they were not seen after the application of any of the other variants. Another possible explanation is that they were highly stained unsaturated lipids, since this method is known to increase the contrast of osmiophilic cellular components (Seligman *et al.*, 1966). The cells in variant 5 were more contrasted than the cells fixed with the control procedure, because the condenser lens setting was at 15 and not 12 (Figs. 3b and 7c). The condenser lens setting changes the beam's effective spot size, which affects both the resolution and, more importantly here, the contrast of the image. Decreasing the condenser lens excitation increases the spot size and probe current interacting with the specimen, resulting in an increased signal being emitted.

## Conclusions

The type of chemical fixation used affected the preservation and contrast of the cells, and the results depended on the type of cell being fixed. The contrast and preservation of both cell types was better following the use of the



OTO method, than when fixatives containing ruthenium red had been applied. The OTO method ensured high contrast of the stress fibres and nuclei at high accelerating voltages, and focal adhesion sites at 4 kV. Another possibility for improving the contrast of the images would be to coat the samples with carbon which has a lower density than Au/Pd.

Another observation made was that filopodia were present on the undersurface of the L929 cells at the interface between the cell and the substrate. These were not observed in c-3T3 cells, suggesting that the focal adhesion areas of the respective cell types are different, in some way. Further studies of the cell adhesion areas could be performed using immunocytochemistry, TEM and interference reflection microscopy in order to investigate whether there is a difference between the adhesion modes of the two cell types.

When using this method, it must be remembered that structures closest to the ventral surface of the cell will predominate in clarity. The work has also shown that using a combination of suitable specimen staining procedures, along with their observation using the HCBSE technique, will aid future detailed study of cellular structures.

#### Acknowledgements

We thank R.Peter for technical assistance with cell culturing. This study was in part supported by the Swiss National Science Foundation grant # 32-4931596.

#### References

- Abraham JL, DeNee PB (1973) Scanning electron microscope histochemistry using backscatter electrons and metal stains. *Lancet* May 19: 1125.
- Aoki M, Tavassoli M (1981) OTO method for preservation of actin filaments in electron microscopy. *J Histochem Cytochem* **29**: 682-683.
- Becker RP, Sogard M (1979) Visualisation of subsurface structures in cells and tissues by backscattered electron imaging. *Scanning Electron Microsc* **1979**; II: 835-870.
- De Bruijn WC (1968) A modified OsO<sub>4</sub> - (double) fixation procedure which selectively contrasts glycogen. *Proc. 4<sup>th</sup> Eur Reg Conf Electron Microsc.* pp 65-66.
- De Bruijn WC (1973) Glycogen, its chemistry and morphologic appearance in the electron microscope. *J Ultrastruct Res* **42**: 29-50.
- Elvin P, Evans CW (1982) The adhesiveness of normal and SV40-transformed BALB/c 3T3 cells: effects of culture density and shear rate. *Eur J Cancer Clin Oncol* **18**: 669-675.
- Glauert AM (1975) Fixation, dehydration and embedding of biological specimens. In: *Practical Methods in Electron Microscopy* vol. 3, Part 1. Glauert AM (ed). Elsevier, Amsterdam.
- Goldstein JI, Newbury DE, Echlin P, Romig AD, Lyman CE, Fiori C, Lifshin E (1992) *Scanning electron microscopy and X-ray microanalysis- a text for biologists, material scientists and geologists* (2<sup>nd</sup>ed). Plenum Press, New York. pp 69-147.
- Hayat MA (1989) *Principles and Techniques of Electron Microscopy - Biological Applications*. Macmillan Press Ltd, London. pp 298
- Kelley RO, Dekker AF, Bluemink JG (1973) Ligand-mediated osmium binding: its application in coating biological specimens for scanning electron microscopy. *J Ultrastruct Res* **45**: 254-258.
- LaFountain JR, Zobel CR, Thomas HR, Galbreath C (1977) fixation and staining of F-actin and microfilaments using tannic acid. *J Ultrastruct Res* **58**: 78-86.
- Luft JH (1971) Ruthenium red and violet. I. Chemistry, purification, methods of use for electron microscopy and mechanism of action. *Anat Rec* **171**: 347-368.
- McDonald K (1984) Osmium ferricyanide fixation improves microfilament preservation and membrane visualisation in a variety of animal cell types. *J Ultrastruct Res* **86**: 107-118.
- Mizuhira V, Futaesaku Y (1972) New fixative for biological membrane using tannic acid. *Acta Histochem Cytochem* **5**: 233-236.
- Palluel P (1947) Composante rediffusee du rayonnement electronique secondaire des metaux. (Diffusion composition of secondary electron rays in metals). *Compt. Rend. Acad Sci (Paris)* **224**: 1492-1494.
- Richards RG, ap Gwynn I (1995) Backscattered electron imaging of the undersurface of resin-embedded cells by field-emission scanning electron microscopy. *J Microsc* **177**: 43-52.
- Richards RG, Rahn BA, ap Gwynn I (1995) Scanning electron microscopy of the undersurface of cell monolayers grown on metallic implants. *J Mat Sci- Mat in Med* **6**: 120-124.
- Richards RG, Owen GRh, Rahn BA, ap Gwynn I (1997) A quantitative method of measuring cell adhesion areas. *Review. Cells and Materials* **7**: 15-30.
- Sabatini DD, Bensch K, Barnett RJ (1963) Cytochemistry and electron microscopy. The preservation of cellular ultrastructure and enzymatic activity by aldehyde fixation. *J Cell Biol* **17**: 19-58.
- Seligman AM, Wasserkrug HL, Hanker JS (1966) A new staining method (OTO) for enhancing contrast of lipid-containing membranes and droplets in osmium tetroxide-fixed tissue with osmiophilic thiocarbo-hydrazide (TCH). *J Cell Biol* **30**: 424-432.
- Simionescu N, Simionescu M (1976) Galloyl-glucoses of low molecular weight as mordant in electron microscopy (1) Procedure and evidence for mordanting effect. *J Cell Biol* **70**: 608-621.

Sobota A, Mrozinska K, Popov VJ (1997) Anionic domains on the cytoplasmic surface of the plasma membrane of *Acanthamoeba castellanii* and their relation to the calcium-binding microregions. *Acta Protozoologica* **36**: 187-196.

Trump B, Bulger R (1966) New ultrastructural characteristics of cells fixed in a glutaraldehyde-osmium tetroxide mixture. *Lab Invest* **15**: 368-379.

Watson ML (1958) Staining of tissues for electron microscopy with heavy metals. *J Biophys Biochem Cytol* **4**: 475-478.

### Discussion with Reviewers

**G.M. Roomans:** The OTO method is designed to increase the amount of osmium binding to particular cellular structures. While this makes these structures easier to see, which certainly is an advantage, it may give rise to unrealistic ideas about the actual size of the structures (e.g., attachment areas), which may be a disadvantage in quantitative studies. Please comment.

**Authors:** In the original paper (Richards *et al.* 1997) on measuring cell adhesion areas a postfixation with 0.5% osmium tetroxide and ruthenium red was used. In this method, where the areas of adhesion were compared, the amount of their staining and the penetration of the electron beam into them was the same in each micrograph, so that comparison could be made. Now that the staining method has been improved, again the comparisons of adhesion should only be made with cell cultures fixed by the same method and observed under the same microscope operating conditions. Only qualitative comparisons could be made with work using other staining methods or slightly different microscope operating conditions.

**A.S.G. Curtis:** The Thermanox coverslips often have appreciable surface debris on them and other defects. Is it possible that at least some of the structures seen outside the cells and possibly some of these seen on the underside of the cells are such defects? For example figure 6e appears to show a regular rippling and there are a number of very black spots, for example in Figs. 6b and 6c which might well be images of things that have nothing to do with the cells.

**Authors:** In Fig. 6e the rippling on the cell (which also can be seen with a black shadow in Fig. 6f) in several places is where the resin has not been removed cleanly from the Thermanox. If there is debris present it should be embedded within the resin and if it is low density Thermanox derived, debris it should not stain or show up with the BSE imaging. The black spots in other images are also areas of resin damage. The damage may initially be caused from debris or other defects that are firmly bound to the Thermanox.

**W.L. Jongbloed:** Why are the cells embedded in LR White instead of Epon or Araldite? LR White is mostly used at low temperatures in immunocytochemistry. At room temperature the preservation capabilities of LR White are not sufficient, due to the release of heat, causing the extraction of certain cytoplasmic components.

**Authors:** Unfortunately Araldite and Spurr bind too strongly to the plastic discs, fracturing them upon removal. We have looked at stained structures using HCBSE imaging with the FESEM in TEM blocks of both LR White and Araldite resins (Richards and ap Gwynn, 1996) and more recently with Spurr resin, but where the technique did not involve having plastic discs as the substrate. The method should also work with Epon resin. We have not observed any obvious artefacts which could have been formed as a result of the exothermic polymerisation of the resin.

**W.L. Jongbloed:** What does “high emission BSE imaging” mean with respect to standard, is it applicable for the various brands of FESEM’s ?

**Authors:** In general, all HCBSE imaging in our laboratory is at 50  $\mu$ A. Our standard for normal imaging with the Hitachi 4100 is 10  $\mu$ A, but settings up to 50  $\mu$ A can be achieved with this microscope and every laboratory uses their own standards of emission current, kV etc. We believe that such work could also be performed with Schottky field emission gun instruments (LEO and Philips) but we are not sure whether or not JEOL instruments can be run with such high emission currents.

**W.L. Jongbloed:** Why did you use a (rather thick) Au/Pd coating, BSE do not show charging?

**Authors:** In this work we used 10 nm, though normally we use 8 nm. Neither settings have reduced the contrast of the BSE image. Using less than 8 nm coating with our system, used at the higher accelerating voltage of 15 kV in HCBSE mode, results in severe damage to the specimen.

**W.L. Jongbloed:** Structures that were probably saturated lipid droplets... Have you done any TEM sectioning and observation of these sections both in TEM and FESEM, the latter in the BSE mode? Could it be that those structures are lysosomes? Lysosomes are often present in large quantities in cell growth wells, quite some hydrolysis by acid phosphatase takes place at cell growth and death.

**Authors:** We have not performed any TEM in this project, since the aim of the project was to improve contrast of focal adhesion areas. We do not think that the structures are lysosomes, which are membrane bound and would stain with osmium. The observed structures clearly did not take up osmium, but had a smooth spherical outline - typical of lipid droplets. This is not a main area of this work.

**W.L. Jongebloed:** Have you used combined SE/BSE imaging as well as a comparison ?

**Authors:** No, since the cells are embedded in resin, the SE image only shows the structure of the resin surface, giving no detail of the underlying material.

#### **Additional References**

Richards RG, ap Gwynn I (1996) A novel method for viewing heavy metal stained and embedded biological tissue by field emission scanning electron microscopy. *Scanning Microsc* **10**: 111-119.